

# Octahedral molybdenum iodide clusters with pyrazole or pyrazolate ligands

Ksenia S. Kozlova,<sup>a,b</sup> Alexey S. Berezin,<sup>a</sup> Natalia V. Kuratieva,<sup>a</sup>  
Michael A. Shestopalov,<sup>a</sup> Anton A. Ivanov<sup>a\*</sup>

<sup>a</sup> Nikolaev Institute of Inorganic Chemistry SB RAS, 3 Acad. Lavrentiev Ave.,  
Novosibirsk 630090, Russian Federation.

<sup>b</sup> Novosibirsk State University, 2 Pirogov Str., 630090 Novosibirsk, Russian  
Federation.

\* Correspondence: [ivanov338@niic.nsc.ru](mailto:ivanov338@niic.nsc.ru)

## TABLE OF CONTENT

<b>Powder X-ray diffraction analysis data</b> .....	3
<b>Single-crystal X-ray diffraction data</b> .....	4
<b>Reactivity: <math>^1\text{H}</math> NMR data</b> .....	6
<b>Luminesce in solution: <math>^1\text{H}</math> NMR data</b> .....	8
<b>TGA data and FTIR spectra</b> .....	9
<b>Crystal structure data</b> .....	12
<b>References</b> .....	13

## Powder X-ray diffraction analysis data

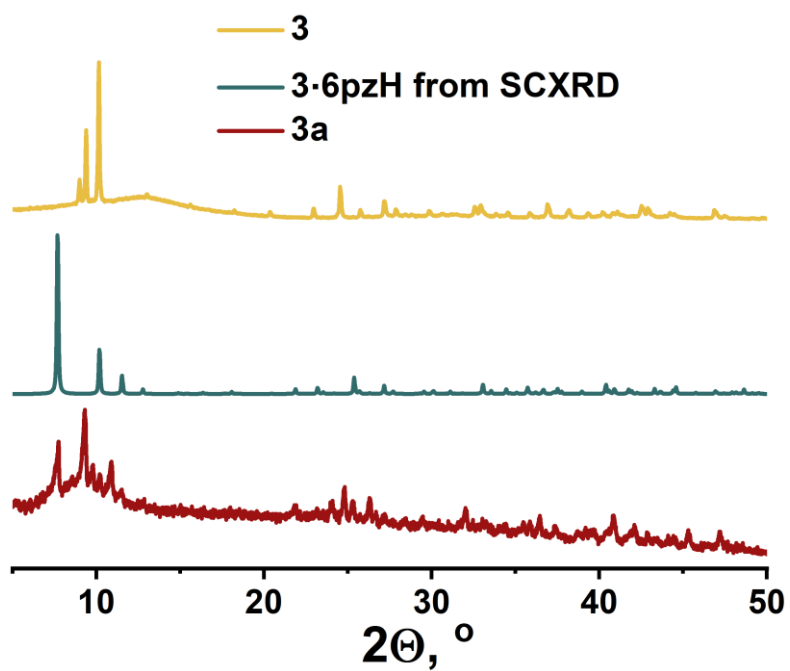


**Figure S1.** Powder X-ray diffraction patterns of **3** and **3a** in comparison with calculated one from the SCXRD data for **3·6pzH**.

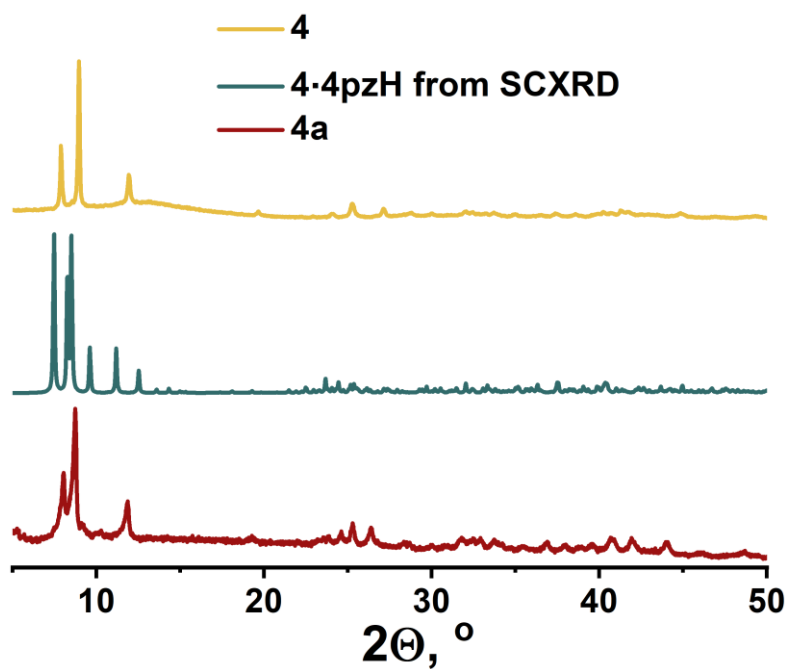


**Figure S2.** Powder X-ray diffraction patterns of **4** and **4a** in comparison with calculated one from the SCXRD data for **4·4pzH**.

## Single-crystal X-ray diffraction data

**Table S1.** Selected crystallographic parameters of the single-crystal X-ray diffraction structural analysis for  $K_2[Mo_6I_8(OH)_6] \cdot 13H_2O$  (**1·13H<sub>2</sub>O**),  $[Mo_6I_8(H_2O)_6](NO_3)_4 \cdot 2H_2O$  (**2·2H<sub>2</sub>O**),  $[K_2[Mo_6I_8(pz)_6] \cdot 6pzH$  (**3·6pzH**),  $[Mo_6I_8(pzH)_6](NO_3)_4 \cdot 4pzH$  (**4·4pzH**) in comparison with literature data.

Cluster	Mo–Mo distances, Å	Mo–I distances, Å	Mo–O distances, Å	Mo–N distances, Å	Ref
<b>1·13H<sub>2</sub>O</b>	2.6536(5) – 2.6738(5)	2.7745(4) – 2.8147(4)	2.098(3) – 2.106(3)	–	This work
<b>2·2H<sub>2</sub>O</b>	2.6469(7) – 2.6652(6)	2.7644(4) – 2.7852(4)	2.150(4) – 2.191(4)	–	This work
$[Mo_6I_8(H_2O)_2(OH)_4] \cdot 2H_2O$	2.6683(8)	2.7896(7) – 2.8092(6)	2.125(4)	–	1
$[Mo_6I_8(H_2O)_2(OH)_4] \cdot 12H_2O$	2.6623(5) – 2.6753(5)	2.7633(4) – 2.7923(4)	2.136(3)	–	1
$[Mo_6I_8(H_2O)_2(OH)_4] \cdot 14H_2O$	2.6533(3) – 2.6730(3)	2.7723(3) – 2.8195(3)	2.085(2) – 2.175(2)	–	1
$[Mo_6I_8(H_2O)_4(OH)_2](NO_3)_2 \cdot 3H_2O$	2.6509(4) – 2.6751(4)	2.7599(4) – 2.8049(4)	2.113(2) – 2.189(3)	–	2
$[Mo_6I_8(H_2O)_4(OH)_2](OTs)_2 \cdot 2H_2O$	2.647(1) – 2.662(1)	2.781(1) – 2.801(1)	2.053(7) – 2.175(8)	–	2
<b>3·6pzH</b>	2.6677(4) – 2.6808(4)	2.7687(4) – 2.7801(3)	–	2.186(3)	This work
<b>4·4pzH</b>	2.6757(3) – 2.6819(3)	2.7522(3) – 2.7782(3)	–	2.216(2) – 2.235(2)	This work
$(Bu_4N)_2[Mo_6I_8(trz)_6]$	2.6645(19) – 2.6973(19)	2.7479(19) – 2.7921(18)	–	2.158(13) – 2.210(14)	3
$Cs_{0.27}[Mo_6I_8(trz)I_5]_{0.27} \cdot cis-[Mo_6I_8(trz)_2I_4]_{0.73}$	2.665(10) – 2.688(8)	2.752(7) – 2.791(10)	–	2.21(2)	4
$(Bu_4N)_2[Mo_6I_8(N_3C_2(COOCH_3)_2)_6]$	2.6721(7) – 2.6794(6)	2.7588(6) – 2.7815(6)	–	2.183(5) – 2.220(4)	5
$(Bu_4N)_2[Mo_6I_8(N_4C-Ph)_6]$	2.6728(10) – 2.6856(9)	2.7588(8) – 2.7768(9)	–	2.230(8) – 2.238(9)	6

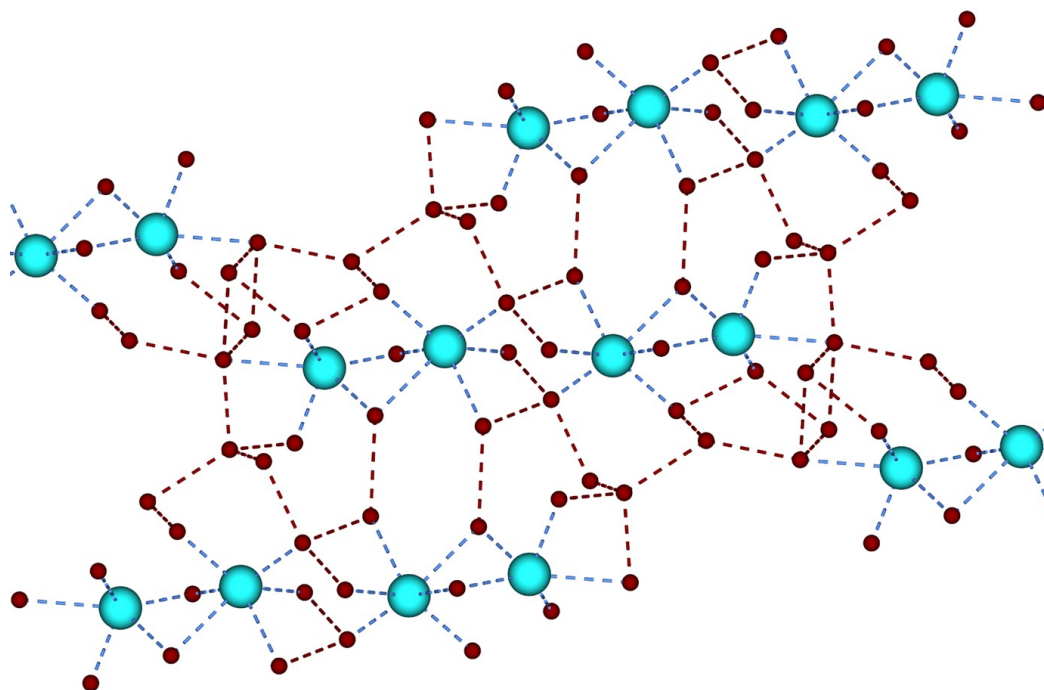


**Figure S3.** Packing of potassium cations in the layers in the crystal structure of **1·13H<sub>2</sub>O**. Color code: O – red, K – cyan, O···O – dashed red, O···K – dashed blue.

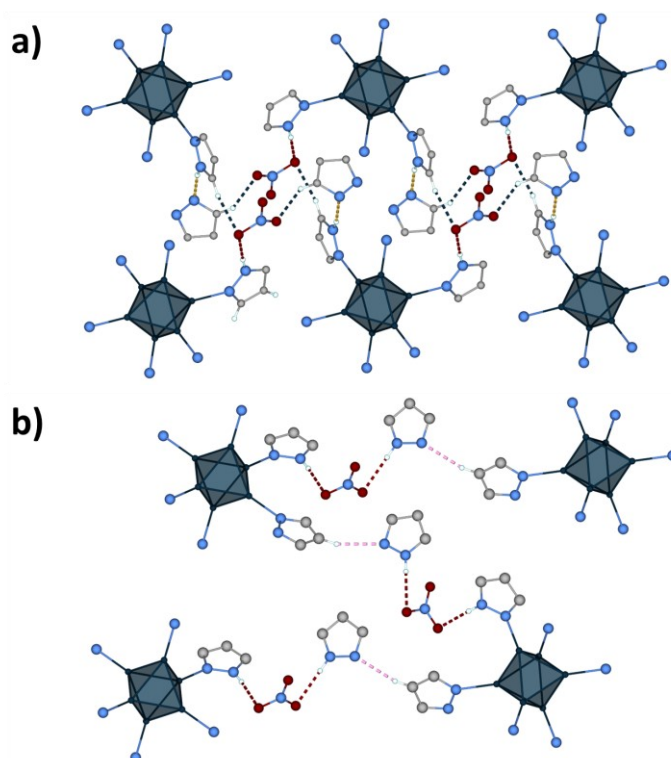


**Figure S4.** Packing in the crystal structure of **4·4pzH**: a) hydrogen bonds forming the layers, b) hydrogen bonds between layers. Color code: Mo – dark blue, N – light blue, O – red, C – gray, H – white, N···H-N – dashed yellow, O···H-N – dashed red, O···H-C – dashed blue, N···H-C – dashed pink.

## Reactivity: $^1\text{H}$ NMR data

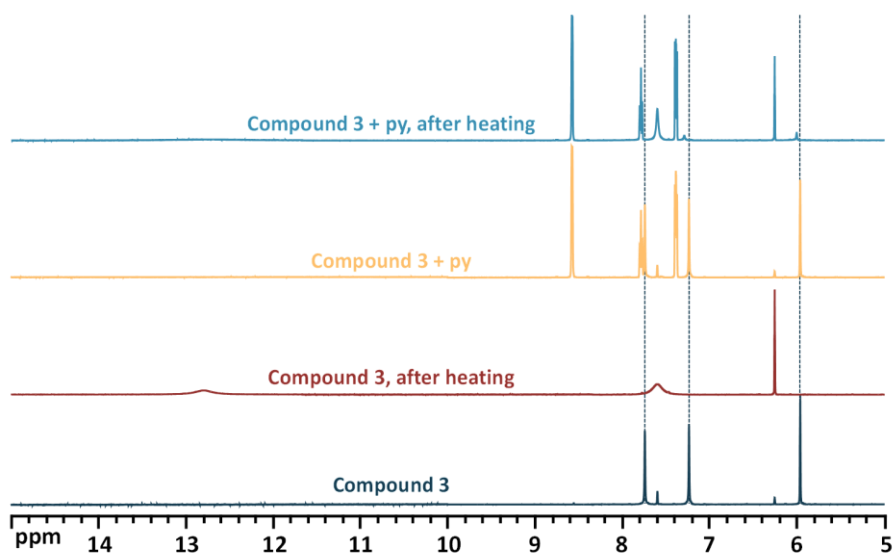


**Figure S5.**  $^1\text{H}$  NMR spectra of compound **3** in  $\text{DMSO-d}_6$  in presence of competing ligands (py = pyridine) and/or under heating at  $100^\circ\text{C}$  for 4 h.

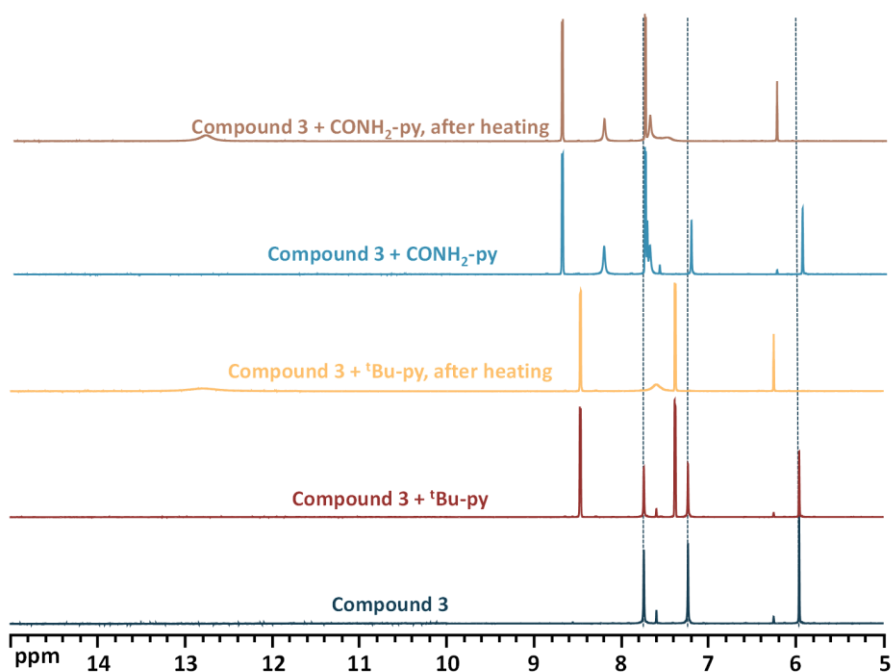


**Figure S6.**  $^1\text{H}$  NMR spectra of compound **3** in  $\text{DMSO-d}_6$  in presence of competing ligands ( $^t\text{Bu}$ -py = 4-tert-butylpyridine,  $\text{CONH}_2$ -py = isonicotinamide) and under heating at  $100^\circ\text{C}$  for 4 h.

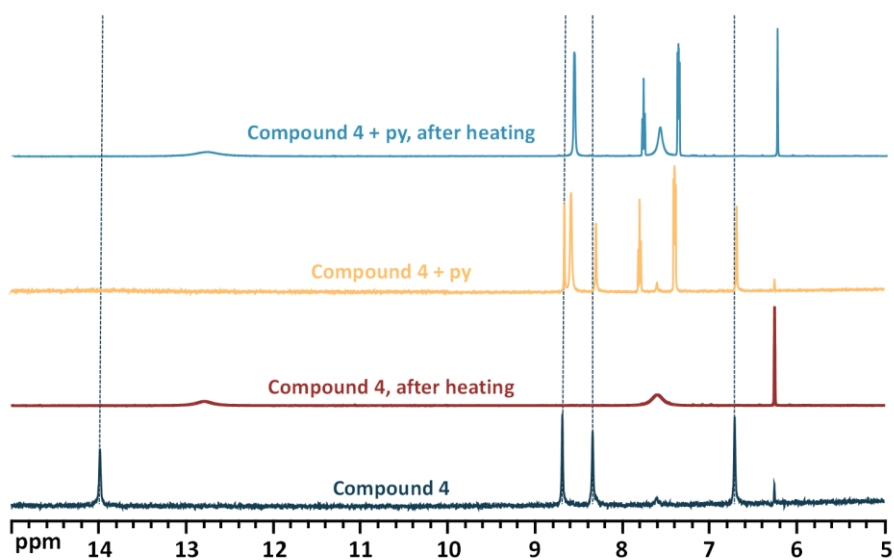


**Figure S7.**  $^1\text{H}$  NMR spectra of compound **4** in  $\text{DMSO-d}_6$  in presence of competing ligands (py = pyridine) and/or under heating at  $100^\circ\text{C}$  for 4 h.

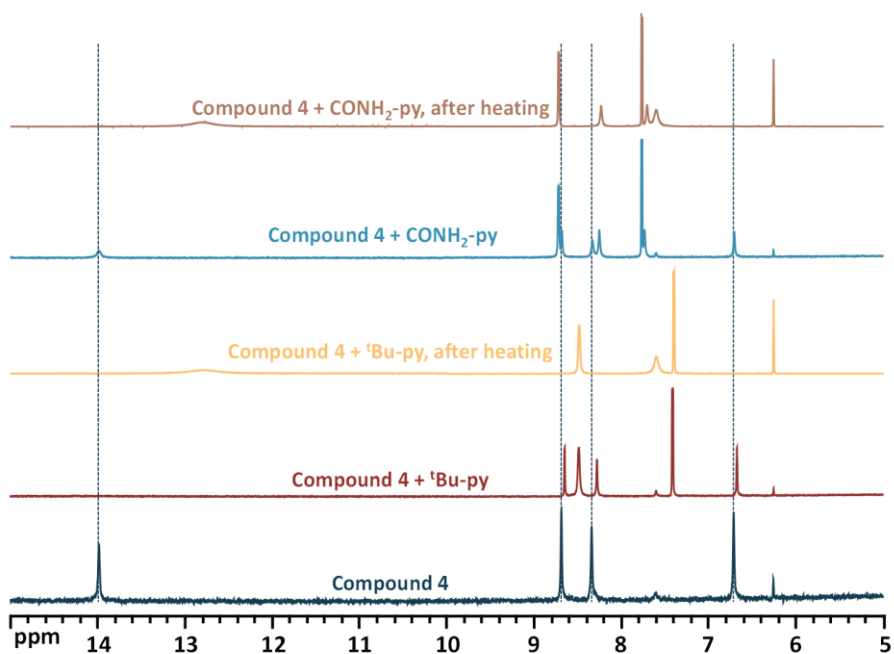


**Figure S8.**  $^1\text{H}$  NMR spectra of compound **4** in  $\text{DMSO-d}_6$  in presence of competing ligands ( $t\text{Bu-py}$  = 4-tert-butylpyridine,  $\text{CONH}_2\text{-py}$  = isonicotinamide) and under heating at  $100^\circ\text{C}$  for 4 h.

## Luminescence in solution: $^1\text{H}$ NMR data

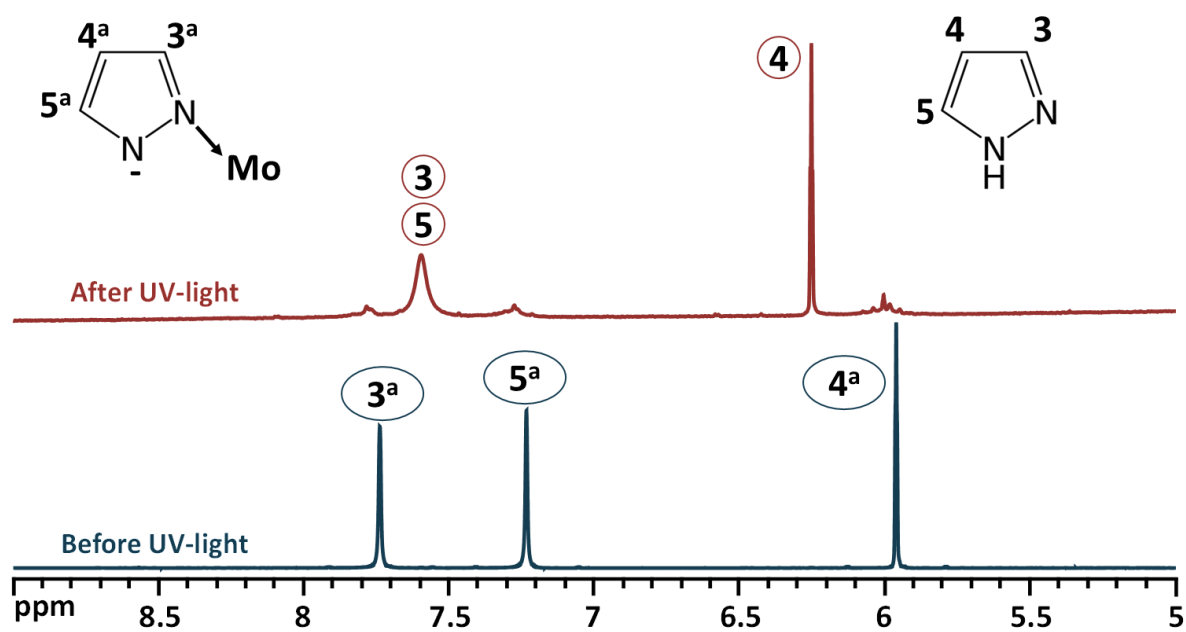


**Figure S9.**  $^1\text{H}$  NMR spectra of DMSO- $d_6$  solution of compound **3** before and after UV irradiation ( $\lambda = 365$  nm).

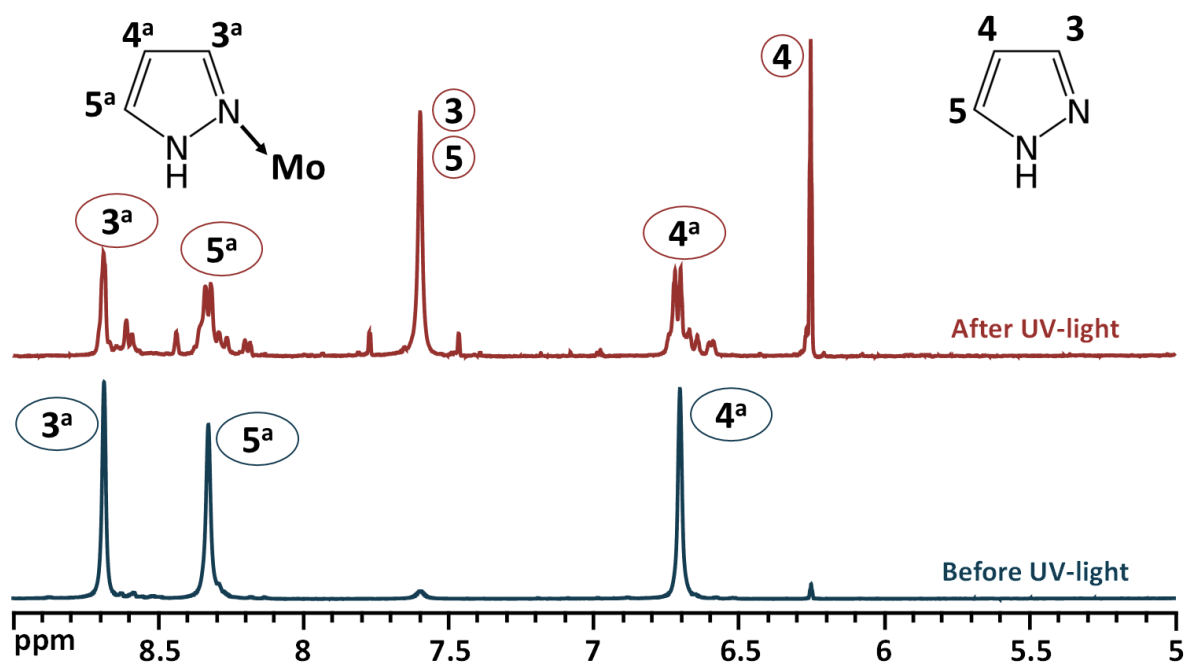


**Figure S10.**  $^1\text{H}$  NMR spectra of DMSO- $d_6$  solution of compound **4** before and after UV irradiation ( $\lambda = 365$  nm).



## TGA data and FTIR spectra

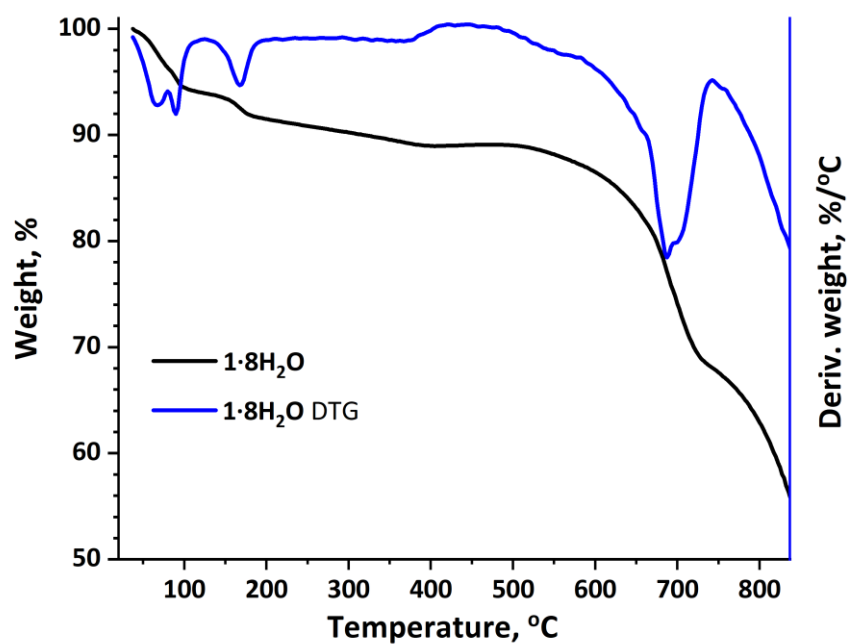


Figure S11. TG and DTG curves of 1·8H<sub>2</sub>O.

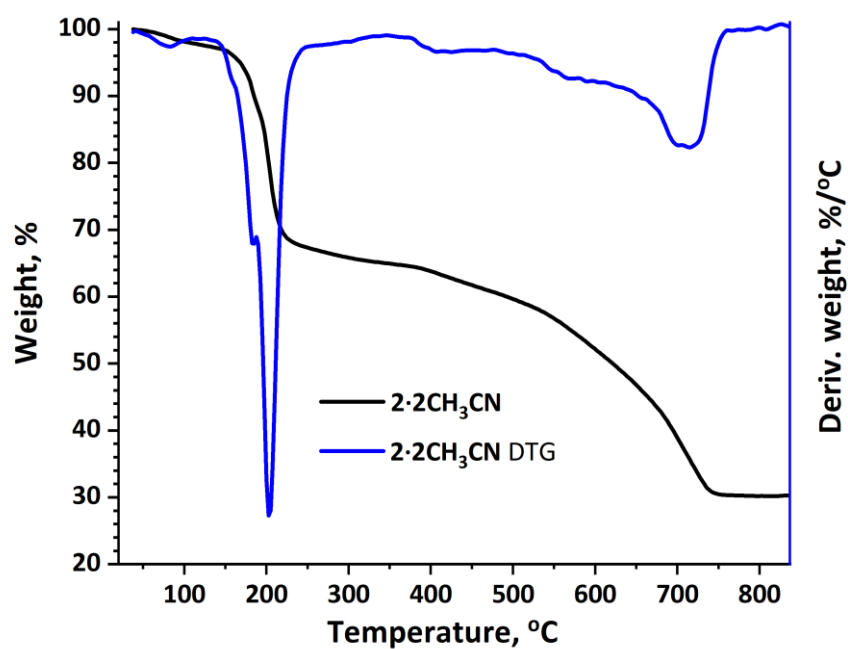


Figure S12. TG and DTG curves of 2·2CH<sub>3</sub>CN.

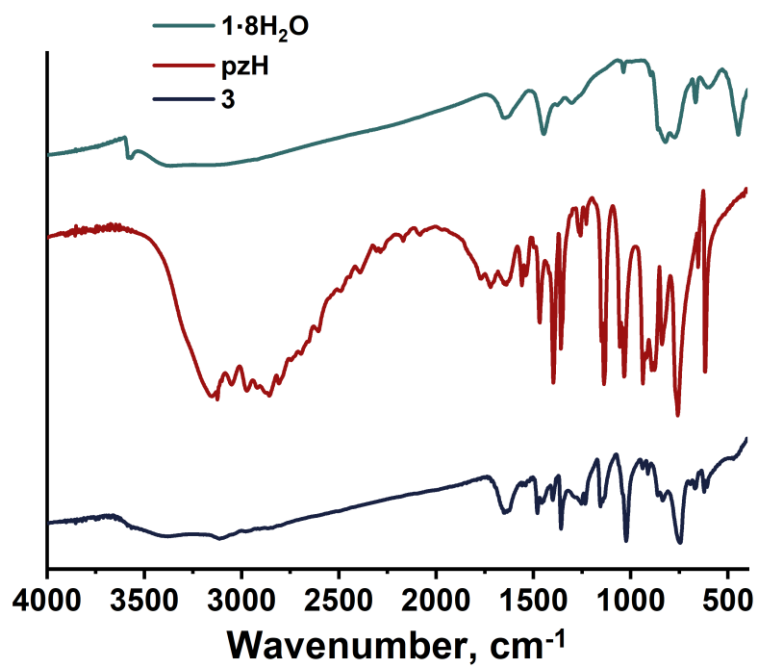


Figure S13. FTIR spectrum of **3** in comparison with pyrazole and 1·8H<sub>2</sub>O.

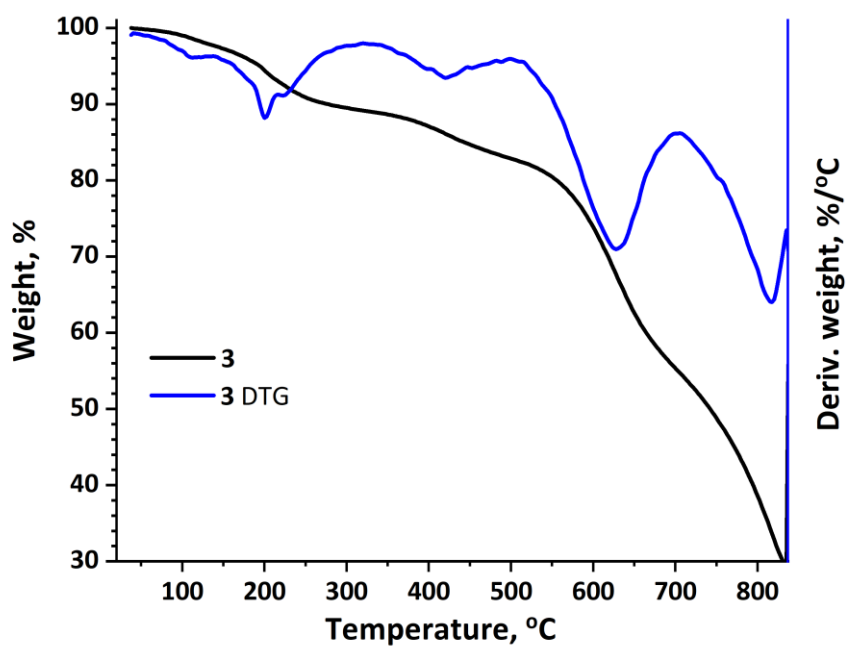


Figure S14. TG and DTG curves of **3**.

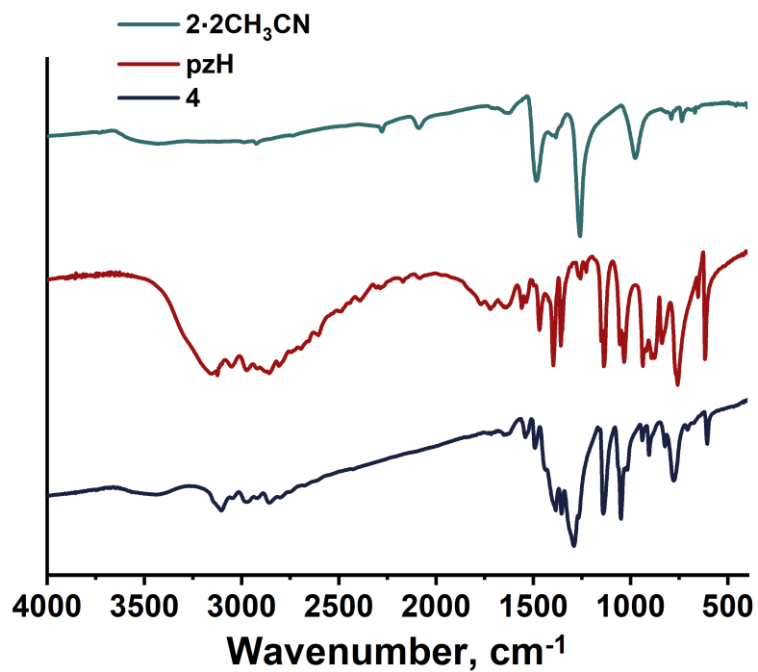


Figure S15. FTIR spectrum of **4** in comparison with pyrazole and 2·2CH<sub>3</sub>CN.

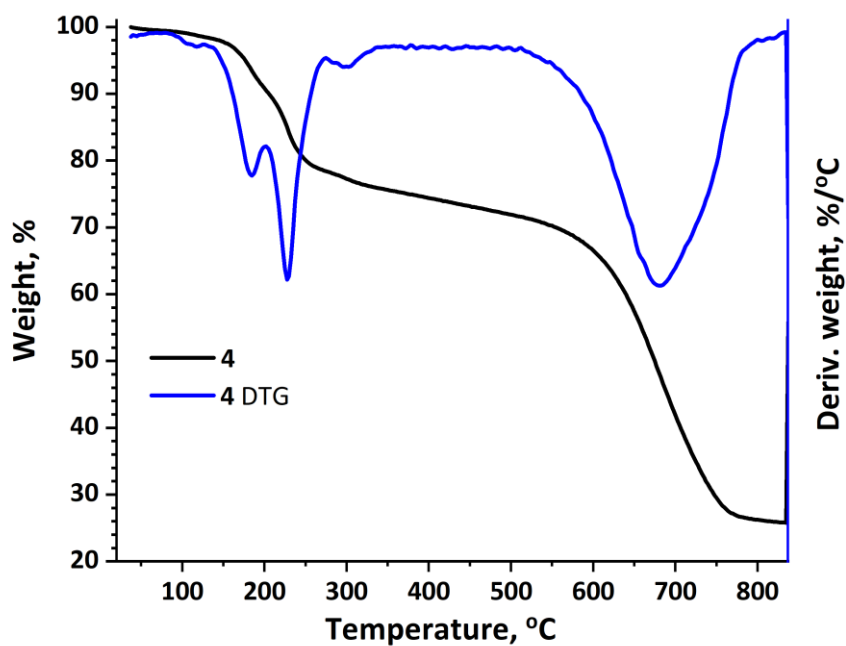


Figure S16. TG and DTG curves of **4**.

## Crystal structure data

**Table S2.** Selected crystallographic parameters of the single-crystal X-ray diffraction structural analysis for  $K_2[Mo_6I_8(OH)_6] \cdot 13H_2O$  (**1·13H<sub>2</sub>O**),  $[Mo_6I_8(H_2O)_6](NO_3)_4 \cdot 2H_2O$  (**2·2H<sub>2</sub>O**),  $K_2[Mo_6I_8(pz)_6] \cdot 6pzH$  (**3·6pzH**),  $[Mo_6I_8(pzH)_6](NO_3)_4 \cdot 4pzH$  (**4·4pzH**).

Compound	<b>1·13H<sub>2</sub>O</b>	<b>2·2H<sub>2</sub>O</b>	<b>3·6pzH</b>	<b>4·4pzH</b>
CCDC	2363823	2363821	2363822	2363824
Empirical formula	H <sub>32</sub> I <sub>8</sub> K <sub>2</sub> Mo <sub>6</sub> O <sub>19</sub>	H <sub>16</sub> I <sub>8</sub> Mo <sub>6</sub> N <sub>4</sub> O <sub>20</sub>	C <sub>36</sub> H <sub>42</sub> I <sub>8</sub> K <sub>2</sub> Mo <sub>6</sub> N <sub>24</sub>	C <sub>30</sub> H <sub>40</sub> I <sub>8</sub> Mo <sub>6</sub> N <sub>24</sub> O <sub>12</sub>
Formula weight	2005.29	1983.01	2479.97	2519.70
Temperature, K	220	150	150	150
Crystal system	Triclinic	Triclinic	Trigonal	Monoclinic
Space group	$P \bar{1}$	$P \bar{1}$	$R \bar{3}$	$P 2_1/n$
<i>a</i> , Å	9.6328(4)	10.5953(2)	17.3571(3)	11.0559(3)
<i>b</i> , Å	11.7341(5)	10.7947(2)	17.3571(3)	11.5527(3)
<i>c</i> , Å	15.9020(7)	15.9552(3)	17.8314(6)	24.1189(6)
$\alpha$ , °	88.590(2)	90.1550(10)	90	90
$\beta$ , °	86.932(2)	90.6780(10)	90	101.3400(10)
$\gamma$ , °	88.658(2)	117.1390(10)	120	90
<i>V</i> , Å <sup>3</sup>	1793.88(13)	1623.75(5)	4652.3(2)	3020.46(14)
<i>Z</i>	2	2	3	2
$\rho_{\text{calc}}$ , g/cm <sup>3</sup>	3.712	4.056	2.656	2.770
$\mu$ , mm <sup>-1</sup>	9.207	9.925	5.343	5.368
F (000)	1796	1760	3420	2320
Crystal size	0.07 × 0.08 × 0.03	0.24 × 0.18 × 0.16	0.08 × 0.07 × 0.03	0.20 × 0.14 × 0.09
$\Theta$ range for data collection, °	2.135 to 31.547	1.276 to 27.604	2.347 to 28.288	2.215 to 34.355
Index ranges	$-14 \leq h \leq 14$ $-17 \leq k \leq 17$ $-23 \leq l \leq 23$	$-13 \leq h \leq 13$ $-14 \leq k \leq 14$ $-20 \leq l \leq 20$	$-20 \leq h \leq 23$ $-23 \leq k \leq 22$ $-23 \leq l \leq 23$	$-17 \leq h \leq 17$ $-18 \leq k \leq 18$ $-33 \leq l \leq 38$
Reflections collected	40283	13976	18111	69472
Independent reflections	11877 [R <sub>int</sub> = 0.0322]	7429 [R <sub>int</sub> = 0.0411]	2572 [R <sub>int</sub> = 0.0369]	12673 [R <sub>int</sub> = 0.0496]
Data/restraints/parameters	11877/0/317	7429/15/353	2572/0/125	12673/18/375
Goodness-of-fit on F <sup>2</sup>	1.036	1.080	1.088	1.068
<i>R</i> <sub>1</sub> / <i>wR</i> <sub>2</sub> ( <i>I</i> > 2 $\sigma$ ( <i>I</i> ))	0.0279/0.0655	0.0333/0.0817	0.0223/0.0448	0.0306/0.0586
<i>R</i> <sub>1</sub> / <i>wR</i> <sub>2</sub> (all data)	0.0363/0.0681	0.0369/0.0836	0.0325/0.0467	0.0505/0.0617
$\Delta\rho_{\text{max}}/\Delta\rho_{\text{min}}$ (e·Å <sup>-3</sup> )	2.546/−2.540	1.448/−1.745	0.571/−0.532	1.377/−1.271

## References

1. M. A. Mikhaylov, P. A. Abramov, V. Y. Komarov and M. N. Sokolov, *Polyhedron*, 2017, **122**, 241-246.
2. M. V. Marchuk, N. A. Vorotnikova, Y. A. Vorotnikov, N. V. Kuratieva, D. V. Stass and M. A. Shestopalov, *Dalton Trans.*, 2021, **50**, 8794-8802.
3. M. A. Mikhaylov, A. S. Berezin, T. S. Sukhikh, D. G. Sheven', N. B. Kompankov and M. N. Sokolov, *J. Struct. Chem.*, 2022, **63**, 2101-2112.
4. A. A. Ulantikov, K. D. Podolets, T. S. Sukhikh, Y. V. Mironov, K. A. Brylev and Y. M. Gayfulin, *Polyhedron*, 2024, **247**, 116737.
5. A. D. Mironova, M. A. Mikhailov, K. A. Brylev, A. L. Gushchin, T. S. Sukhikh and M. N. Sokolov, *New J. Chem.*, 2020, **44**, 20620-20625.
6. A. Mironova, A. Gushchin, P. Abramov, I. Eltsov, A. Ryadun and M. Sokolov, *Polyhedron*, 2021, **205**, 115282.